Prediction of Viscoelastic Behavior of Blood Flow in Plaque Deposited Capillaries

MUHAMMAD ANWAR SOLANGI*, BAQER SHAH, AND AHSANULLAH BALOCH*****

RECEIVED ON 18.05.2012 ACCEPTED ON 18.09.2012

ABSTRACT

The paper investigates the viscoelastic behaviour of blood over low value of elasticity, to analyse the influence of inertia in the presence of elasticity. For viscoelastic fluids shear-thinning and strain-softening PTT (Phan-Thien/Tanner) constitutive model is employed to identify the influence of elasticity. The computational method adopted is based on a finite element semi-implicit time stepping Taylor-Galerkin/pressure-correction scheme. Simulations are conducted via atherosclerotic vessels along with various percentages of deposition at distinct values of Reynolds numbers. The numerical simulations are performed for recirculation flow structure and development of recirculation length to investigate the impact of atherosclerosis on partially blocked plaque deposited vessels.

Key Words: **Viscoelastic, Non-Newtonian, Atherosclerosis, Blood Flow, Capillaries.**

1. INTRODUCTION

The predictions on viscoelastic behaviour of blood are presented by employing shear thinning and strain softening PTT constitutive model. The viscoelastic behaviour of blood in plaque deposited capillary segment is observed, when the diameter of the capillary blood vessel is smaller than the diameter of red blood cells. Literature review suggests that the micro structure of red blood cells adopt two qualitatively distinct responses to flow. In the first case inelastic Non-Newtonian behaviour is observed at shear rate greater than $3S^{-1}$, while passing through this situation red blood cells deforms but not aggregate and squeezes and move in a single line to pass the artery in two phases, one being the blood cells and the other being plasma. Whereas, at low shear rates ($0\text{-}1S^{-1}$) the red cells deform and form extended aggregates called reuleaux, second case of response of red blood cells is referred as viscoelastic. The tight interaction between the red cells and a thin layer of endothelial cells (present on the wall of the blood vessel, which cannot move but can deform) imposes high shear stresses on the vessel wall. As the shear rate is increased, the aggregates are broken up in to small aggregates and a corresponding decrease in viscosity is observed. In this scenario viscosity of blood decreases with increased shear rate, hence the non-Newtonian effects are added in the form of elasticity and shearing thinning [1].

The prediction of viscoelastic behaviour of blood in capillaries, having an axially symmetric deposition of plaque, presents a considerable challenge to researchers

* Assistant Professor, Department of Basic Sciences & Related Studies, Mehran University of Engineering & Technology, Jamshoro.
** Lecturer, Department of Mathematics, Shah Abdul Latif University, Khairpur Mirs, Sindh.
*** Professor, Department of Basic Sciences & Related Studies, Mehran University of Engineering & Technology, Jamshoro.

as well as medical device design and treatment. To study the viscoelastic nature of blood is more complicated than the Newtonian one. The present study is concerned with the main issues, which arise in numerical simulation of complex viscoelastic flows in two dimensional partially plaque deposited capillaries.

The non-Newtonian behaviour of blood over low value of elasticity is investigated along with governing elongational parameters and inertia. For viscoelastic fluids shear thinning and strain softening PTT constitutive model is employed to identify the influence of rheological variations [2-3]. Flow of blood along with the partially plaque deposited capillaries involving flow separation and reattachment is of considerable technical interest for researchers. Literature review suggests that over the past few years, real fluids study has become a leading issue especially in biomedical, chemical, pharmaceutical and food industries, because of severe limitations for the application of flow theory associated with the flow problems in these industries [4-5]. It has been observed that Newtonian behaviour of blood presents the predictions of several interesting features of blood flow. For example, it is known that the stream line pattern of the recirculation flow region increases in the downstream area as the Reynolds numbers or deposition of plaque increases. Whereas in literature viscoelastic behaviour of blood has received scant attention in comparison to Newtonian flow of blood [6-9].

2. THE PTT CONSTITUTIVE EQUATION

The constitutive equation for the modified PTT differential model with a single relaxation time λ_1, the elastic stress tensor may be expressed as:

$$\lambda_1 \overset{\nabla}{\tau} + f\tau = 2\mu_1 d \tag{1}$$

The total viscosity $\mu=\mu_1+\mu_2$ and the ratio μ_1/μ_2 is 1/9 selected. The non-linear function f, for the exponential case, is:

$$f = e^{\frac{\in\lambda_1}{\mu_1} Tr(\tau)} \tag{2}$$

and for the linear case:

$$f = 1 + \frac{\in\lambda_1}{\mu_1} Tr(\tau) \tag{3}$$

Here $Tr(\tau)$ is the trace of the stress tensor and $\in$ is the material parameter. Shear and elongational properties are controlled by material parameters, $\in$ and μ_1 respectively, which can be evaluated by fitted the linear or exponential data.

3. GOVERNING SYSTEM OF EQUATIONS

The axi-symmetric flow of incompressible viscoelastic nature of blood in the plaque deposited capillary segment can be mathematically modelled through a system comprising mass conversion, momentum transport and viscoelastic stress constitutive equations [10]. These governing equations for two dimensional cylindrical polar coordinates taken over domain Ω, in the absence of body force are given as under:

Continuity Equation:

$$\frac{\partial v_r}{\partial r} + \frac{v_r}{r} + \frac{\partial v_z}{\partial z} = 0 \tag{4}$$

Momentum Equation:

$$r: \ \rho \frac{Dv_r}{Dt} = \left(\frac{\partial}{\partial r} + \frac{1}{r}\right) T_{rr} + \frac{\partial}{\partial z} T_{rz} - \frac{T_{\theta\theta}}{r} - \frac{\partial p}{\partial r} \tag{5}$$

$$z: \ \rho \frac{Dv_z}{Dt} = \left(\frac{\partial}{\partial r} + \frac{1}{r}\right) T_{rz} + \frac{\partial}{\partial z} T_{zz} - \frac{\partial p}{\partial z} \tag{6}$$

Where,

$$T_{rr} = \tau_{rr} + 2\mu_2 \frac{\partial v_r}{\partial r} \tag{7}$$

$$T_{rz} = \tau_{rz} + \mu_2 \left(\frac{\partial v_r}{\partial z} + \frac{\partial v_z}{\partial r} \right) \tag{8}$$

$$T_{zz} = \tau_{zz} + 2\mu_2 \frac{\partial v_z}{\partial z} \tag{9}$$

$$T_{\theta\theta} = \tau_{\theta\theta} + 2\mu_2 \frac{v_r}{r} \tag{10}$$

Constitutive Equations for Exponential Form of PTT Model:

$$\begin{aligned} rr:\ \lambda_1 \frac{\partial \tau_{rr}}{\partial t} &= 2\mu_1 \frac{\partial v_r}{\partial r} - \tau_{rr} \left\{ e^{\frac{\varepsilon \lambda_1}{\mu_1} tr(\tau)} \right\} \\ &- \lambda_1 \left\{ \begin{array}{l} v_r \dfrac{\partial \tau_{rr}}{\partial r} + v_z \dfrac{\partial \tau_{rr}}{\partial z} \\ -2\left(\dfrac{\partial v_r}{\partial r} \tau_{rr} + \dfrac{\partial v_r}{\partial z} \tau_{rz} \right) \end{array} \right\} \end{aligned} \tag{11}$$

$$\begin{aligned} rz:\lambda_1 \frac{\partial \tau_{rz}}{\partial t} &= \mu_1 \left(\frac{\partial v_r}{\partial z} + \frac{\partial v_z}{\partial r} \right) - \tau_{rz} \left\{ e^{\frac{\varepsilon \lambda_1}{\mu_1} tr(\tau)} \right\} \\ &- \lambda_1 \left\{ \begin{array}{l} v_r \dfrac{\partial \tau_{rz}}{\partial r} + v_z \dfrac{\partial \tau_{rz}}{\partial z} - \dfrac{\partial v_r}{\partial r} \tau_{rz} - \dfrac{\partial v_r}{\partial z} \tau_{zz} \\ -\tau_{rz} + \dfrac{\partial v_z}{\partial r} \tau_{rr} - \tau_{rz} + \dfrac{\partial v_z}{\partial z} \tau_{rz} \end{array} \right\} \end{aligned} \tag{12}$$

$$\begin{aligned} zz:\ \lambda_1 \frac{\partial \tau_{zz}}{\partial t} &= 2\mu_1 \frac{\partial v_z}{\partial z} - \tau_{zz} \left\{ e^{\frac{\varepsilon \lambda_1}{\mu_1} tr(\tau)} \right\} \\ &- \lambda_1 \left\{ \begin{array}{l} v_r \dfrac{\partial \tau_{zz}}{\partial r} + v_z \dfrac{\partial \tau_{zz}}{\partial z} \\ -2\left(\dfrac{\partial v_z}{\partial r} \tau_{rz} + \dfrac{\partial v_z}{\partial z} \tau_{zz} \right) \end{array} \right\} \end{aligned} \tag{13}$$

$$\begin{aligned} \theta\theta:\ \lambda_1 \frac{\partial \tau_{\theta\theta}}{\partial t} &= 2\mu_1 \frac{v_r}{r} - \tau_{\theta\theta} \left\{ e^{\frac{\varepsilon \lambda_1}{\mu_1} tr(\tau)} \right\} \\ &- \lambda_1 \left\{ v_r \frac{\partial \tau_{\theta\theta}}{\partial r} + v_z \frac{\partial \tau_{\theta\theta}}{\partial z} - 2\frac{v_r}{r} \tau_{\theta\theta} \right\} \end{aligned} \tag{14}$$

3.1 Non-Dimensional System of Equations

Casting above system of equations into dimensionless form by placing non-dimensional variables along suitable scales as under:

$$r^* = \frac{r}{R}, z^* = \frac{z}{R}, v_r^* = \frac{v_r}{V}, v_z^* = \frac{v_z}{V}, t^* = t\frac{V}{R}, p^* = \frac{p}{\rho V^2}$$

$$\lambda_1^* = \lambda_1 \frac{V}{R}, \mu_i^* = \frac{\mu_i}{\mu}, \tau^* = \frac{\tau}{\rho V^2}$$

Where V and R are considered as characteristic velocity and length respectively, V is taken as velocity of blood and R is taken as radius of artery respectively. Whereas ν_r and ν_z are the velocity components in r and z direction, τ is the extra stress tensor, p is the pressure of blood, λ_1 is the relaxation time, ρ is the density of blood, t is the time and μ is the constant viscosity given by $\mu=\mu_1+\mu_2$, here μ_1 is the elastic solute viscosity and μ_2 is the Newtonian solvent viscosity. By substituting these non-dimensional values in Equations (4-6) and Equations (11-14), then discarding asterisks for brevity and simplicity, the above system of equations may be rewritten as:

Continuity Equation:

$$\frac{\partial v_r}{\partial r} + \frac{v_r}{r} + \frac{\partial v_z}{\partial z} = 0 \tag{15}$$

Momentum Equations:

$$\begin{aligned} r:\ R_e \frac{d v_r}{dt} &= \left[\frac{\partial}{\partial r}\left(2\mu_2 \frac{\partial v_r}{\partial r} \right) + \frac{\partial}{\partial z}\left\{ \mu_2 \left(\frac{\partial v_r}{\partial z} + \frac{\partial v_z}{\partial r} \right) \right\} + \frac{2\mu_2}{r}\left(\frac{\partial v_r}{\partial r} - \frac{v_r}{r} \right) \right] \\ &+ \left(\frac{\partial}{\partial r} + \frac{1}{r} \right)\tau_{rr} + \frac{\partial \tau_{rz}}{\partial z} - \frac{\tau_{\theta\theta}}{r} - \mathrm{Re}\left\{ v_r \frac{\partial v_r}{\partial r} + v_z \frac{\partial v_z}{\partial z} \right\} - \frac{\partial p}{\partial r} \end{aligned} \tag{16}$$

$$z:\ R_e\frac{dv_z}{dt}=\left[\frac{\partial}{\partial r}\left\{\mu_2\left(\frac{\partial v_r}{\partial z}+\frac{\partial v_z}{\partial r}\right)\right\}+\frac{\partial}{\partial z}\left\{\left(2\mu_2\frac{\partial v_z}{\partial z}\right)+\frac{\mu_2}{r}\left(\frac{\partial v_r}{\partial z}+\frac{v_r}{r}\right)\right\}\right]$$
$$+\left(\frac{\partial}{\partial r}+\frac{1}{r}\right)\tau_{rz}+\frac{\partial\tau_{zz}}{\partial z}-\mathrm{Re}\left\{v_r\frac{\partial v_z}{\partial r}+v_z\frac{\partial v_z}{\partial z}\right\}-\frac{\partial p}{\partial r} \tag{17}$$

Where, Re is defined as:

$$\mathrm{Re}=\rho\frac{VR}{\mu}$$

Constitutive Equations:

$$rr:\ W_e\frac{\partial\tau_{rr}}{\partial t}=2\mu_1\frac{\partial v_r}{\partial r}-\tau_{rr}\left\{e^{\frac{\varepsilon W_e}{\mu_1}tr(\tau)}\right\}$$
$$-W_e\left\{v_r\frac{\partial\tau_{rr}}{\partial r}+v_z\frac{\partial\tau_{rr}}{\partial z}-2\left(\frac{\partial v_r}{\partial r}\tau_{rr}+\frac{\partial v_r}{\partial z}\tau_{rz}\right)\right\} \tag{18}$$

$$rz:\ W_e\frac{\partial\tau_{rz}}{\partial t}=2\mu_1\frac{\partial v_r}{\partial r}-\tau_{rr}\left\{e^{\frac{\varepsilon W_e}{\mu_1}tr(\tau)}\right\}$$
$$-W_e\left\{v_r\frac{\partial\tau_{rz}}{\partial r}+v_z\frac{\partial\tau_{rz}}{\partial z}-\frac{\partial v_r}{\partial r}\tau_{rz}-\frac{\partial v_r}{\partial z}\tau_{zz}-\frac{\partial v_z}{\partial r}\tau_{rr}-\frac{\partial v_z}{\partial z}\tau_{rz}\right\} \tag{19}$$

$$zz:\ W_e\frac{\partial\tau_{zz}}{\partial t}=2\mu_1\frac{\partial v_z}{\partial z}-\tau_{zz}\left\{e^{\frac{\varepsilon W_e}{\mu_1}tr(\tau)}\right\}$$
$$-W_e\left\{v_r\frac{\partial\tau_{zz}}{\partial r}+v_z\frac{\partial\tau_{zz}}{\partial z}-2\left(\frac{\partial v_z}{\partial r}\tau_{rz}+\frac{\partial v_z}{\partial z}\tau_{zz}\right)\right\} \tag{20}$$

$$\theta\theta:\ W_e\frac{\partial\tau_{\theta\theta}}{\partial t}=2\mu_1\frac{v_r}{r}-\tau_{\theta\theta}\left\{e^{\frac{\varepsilon W_e}{\mu_1}tr(\tau)}\right\}$$
$$-W_e\left\{v_r\frac{\partial\tau_{\theta\theta}}{\partial r}+v_z\frac{\partial\tau_{\theta\theta}}{\partial z}-2\frac{v_r}{r}\tau_{\theta\theta}\right\} \tag{21}$$

Here $W_e=\lambda^*_1$, referred as Weissenberg number.

4. NUMERICAL METHOD

The numerical scheme adopted here is a semi-implicit Taylor-Galerkin/pressure-correction scheme. This method is based on time stepping procedure, that semi discretises the temporial domain, by applying Taylor series expansion in time and a pressure correction procedure to extract a time stepping scheme of second order accuracy [11-15].

5. DISCRETE SYSTEM OF EQUATIONS

The governing system of equations for the semi-implicit Taylor-Galerkin/pressure-correction scheme is given as:

Momentum Equations:

$$r:\ \frac{2\,\mathrm{Re}}{\Delta t}\left(v_r^{n+\frac{1}{2}}-v_r^n\right)$$
$$=\left[\frac{\partial}{\partial r}\left(2\mu_2\frac{\partial v_r}{\partial r}\right)++\frac{\partial}{\partial z}\left\{\mu_2(\frac{\partial v_r}{\partial z}+\frac{\partial v_z}{\partial r})\right\}+\frac{\partial\mu_2}{r}\left(\frac{v_z}{r})\right)\right]^n$$
$$\left[+\left(\frac{\partial}{\partial r}+\frac{1}{r}\right)\tau_{rz}+\frac{\partial\tau_{rz}}{\partial z}-\frac{\tau_{\theta\theta}}{r}-\mathrm{Re}\left(v_r\frac{\partial v_r}{\partial r}+v_z\frac{\partial v_r}{\partial z})\right)-\frac{\partial p}{\partial r}\right]^n \tag{22}$$

$$z:\ \frac{2\,\mathrm{Re}}{\Delta t}\left(v_z^{n+\frac{1}{2}}-v_z^n\right)$$
$$=\left[\frac{\partial}{\partial r}\left\{\mu_2\left(\frac{\partial v_r}{\partial z}+\frac{\partial v_z}{\partial r}\right)\right\}+\frac{\partial}{\partial z}\left(2\mu_2\frac{\partial v_z}{\partial z}\right)+\frac{\mu_2}{r}\left(\frac{\partial v_r}{\partial z}+\frac{\partial v_z}{\partial r}\right)\right]^n$$
$$\left[+\left(\frac{\partial}{\partial r}+\frac{1}{r}\right)\tau_{rz}+\frac{\partial\tau_{zz}}{\partial z}-\mathrm{Re}\left(v_r\frac{\partial v_z}{\partial r}+v_z\frac{\partial v_z}{\partial z}\right)-\frac{\partial p}{\partial r}\right]^n \tag{23}$$

The fully discrete semi-implicit system of equations in a weak form is written as:

$$r:\ \frac{2\,\mathrm{Re}}{\Delta t}M\left(v_r^{n+\frac{1}{2}}-v_r^n\right)=$$
$$\begin{bmatrix}-\left\{\left(S_3^t-S_4\right)v_r+\left(S_5-S_2^t\right)v_z\right\}+D_1T_{rz}\\+D_2T_{zz}+DT_{rz}-N(V)v_z+L_2p_k\end{bmatrix}^n \tag{24}$$

$$z:\ \frac{2\,\mathrm{Re}}{\Delta t}M(v_z^{n+\frac{1}{2}}-v_z^n)=$$
$$\begin{bmatrix}-\left\{\left(S_3^t-S_4\right)v_r+\left(S_5-S_2^t\right)v_z\right\}+D_1T_{rz}\\+D_2T_{zz}+DT_{rz}-N(V)v_z+L_2p_k\end{bmatrix}^n \tag{25}$$

$$rr: \frac{2We}{\Delta t} M \left(T_{rr}^{n+\frac{1}{2}} - T_{rr}^{n} \right) = \begin{bmatrix} 2\mu_1 D_1 V_r - f\, M\, T_{rr} \\ -We \left\{ N(V)\, T_{rr} - 2\, E_1\, V_r \right\} \end{bmatrix}^n \tag{26}$$

$$rz: \frac{2We}{\Delta t} M \left(T_{rz}^{n+\frac{1}{2}} - T_{rz}^{n} \right) = \begin{bmatrix} \mu_1 \left(D_1 V_r + D_2 V_z \right) - f\, M\, T_{rz} \\ -We \left\{ N(V)\, T_{rz} - E_2\, V_r - E_1\, V_z \right\} \end{bmatrix}^n \tag{27}$$

$$zz: \frac{2We}{\Delta t} M \left(T_{zz}^{n+\frac{1}{2}} - T_{zz}^{n} \right) = \left[2\mu_1 D_2 V_z - f\, M\, T_{rz} - We \left\{ N(V)\, T_{zz} - 2\, E_2\, V_z \right\} \right]^n \tag{28}$$

$$\theta\theta: \frac{2We}{\Delta t} M \left(T_{\theta\theta}^{n+\frac{1}{2}} - T_{\theta\theta}^{n} \right) = \left[\frac{2\mu_1}{r} M\, V_r - f\, M\, T_{\theta\theta} - We \left\{ N(V)\, T_{\theta\theta} - \frac{2}{r} N_1(V)\, T_{\theta\theta} \right\} \right]^n \tag{29}$$

The system of matrices is defined as:

Mass matrix:

$$M = \int_\Omega \Phi_i \Phi_j \, d\Omega \tag{30}$$

Gradient matrices:

$$D = \int_\Omega \frac{\Phi_i \Phi_j}{r} \, d\Omega \tag{31}$$

$$D_1 = \int_\Omega \Phi_i \frac{\partial \Phi_j}{\partial r} \, d\Omega \tag{32}$$

$$D_2 = \int_\Omega \Phi_i \frac{\partial \Phi_j}{\partial z} \, d\Omega \tag{33}$$

Non-linear elastic matrices:

$$E_1 = \int_\Omega \Phi_i \left(\Phi_j T_{rr} \frac{\partial \Phi_j}{\partial r} + \Phi_j T_{rz} \frac{\partial \Phi_j}{\partial z} \right) d\Omega \tag{34}$$

$$E_2 = \int_\Omega \Phi_i \left(\Phi_j T_{rz} \frac{\partial \Phi_j}{\partial r} + \Phi_j T_{zz} \frac{\partial \Phi_j}{\partial z} \right) d\Omega \tag{35}$$

Non-linear advection matrices:

$$N(V) = \int_\Omega \Phi_i \left(\Phi_l V_r^l \frac{\partial \Phi_j}{\partial r} + \Phi_l V_z^l \frac{\partial \Phi_j}{\partial z} \right) d\Omega \tag{36}$$

$$N_1(V) = \int_\Omega \Phi_i \Phi_l V_r^l \Phi_j \, d\Omega \tag{37}$$

$$L_1 = \int_\Omega \frac{\partial \Phi_i}{\partial r} \psi_k \, d\Omega \tag{38}$$

$$L_2 = \int_\Omega \frac{\partial \Phi_i}{\partial z} \psi_k \, d\Omega \tag{39}$$

Momentum diffusion matrices:

$$S_1 = \int_\Omega \mu_2 \left(2 \frac{\partial \Phi_i}{\partial r} \frac{\partial \Phi_j}{\partial r} + \frac{\partial \Phi_i}{\partial z} \frac{\partial \Phi_j}{\partial z} \right) d\Omega \tag{40}$$

$$S_2 = \int_\Omega \frac{\mu_2}{r} \frac{\partial \Phi_i}{\partial r} \Phi_j \, d\Omega \tag{41}$$

$$S_3 = \int_\Omega \frac{\partial \Phi_i}{\partial z} \frac{\partial \Phi_j}{\partial r} \, d\Omega \tag{42}$$

$$S_4 = \int_\Omega \frac{\mu_2}{r} \Phi_i \frac{\partial \Phi_j}{\partial z} \, d\Omega \tag{43}$$

$$S_5 = \int_\Omega \mu_2 \left(\frac{\partial \Phi_i}{\partial r} \frac{\partial \Phi_j}{\partial r} + 2 \frac{\partial \Phi_i}{\partial z} \frac{\partial \Phi_j}{\partial z} \right) d\Omega \tag{44}$$

6. INITIAL AND BOUNDARY CONDITIONS

To obtain the steady state solution, simulations are started with quiescent initial conditions for fixed levels of inertia and elasticity parameters. For the modelling of two dimensional viscoelastic behaviour of blood, the analytic solution of [16], axial velocity profile is fixed at both inlet and outlet, vanishing on solid wall and free on axis of symmetry; vanishing cross component of velocity everywhere; pressure is fixed at only outlet and stresses only at inlet boundary.

7. RESULTS AND DISCUSSION

Numerical computations are carried out by employing PTT model at distinct values of Reynolds numbers being set at Re=100, 200 and 300 respectively along various percentages of deposition i.e. 30, 50 and 70% respectively, in a capillary segment having viscoelasticity value W_e=0.01. The computational predictions are computed in terms of velocity gradients, first normal stress difference, shear stress, vorticity and stream function, so that reattachment length and recirculation flow region of blood to be determined.

In Figs. 3-5 streamline projections are displayed to investigate the impact of inertia in a plaque deposited capillary segment. It is illustrated that blood inertia generates the formation of vortex even at low Reynolds number. Further it is observed that the reattachment length is a function of Reynolds number and deposition level and is having an increasing linear trend along inertia and level of deposition. Furthermore, it is observed that, vortex formed at 30% level of deposition is negligible, moderate at 50% and dominates at 70% level of deposition in the downstream of the capillary segment.

The reattachment length verses Reynolds number at different percentages of deposition levels is computed and presented in Fig. 1. Linear growth of reattachment length is observed with small slope at 60% level of deposition, where as beyond 60% deposition level, reattachment length increases, with the same linear trend with a very high slope, along larger values of Reynolds number.

Developed empirical equations for reattachment length are listed in Table 1, presents linear trend and increases along Reynolds numbers for various levels of deposition. Whereas, polynomial trend of second order is observed in Table 2, which presents empirical equations of reattachment length verses various levels of deposition for different values of Reynolds numbers.

The computed recirculation flow rate of blood against various Reynolds numbers for different levels in percentages is computed and its behaviour is illustrated in Fig. 2. It is observed that the recirculation flow rate of

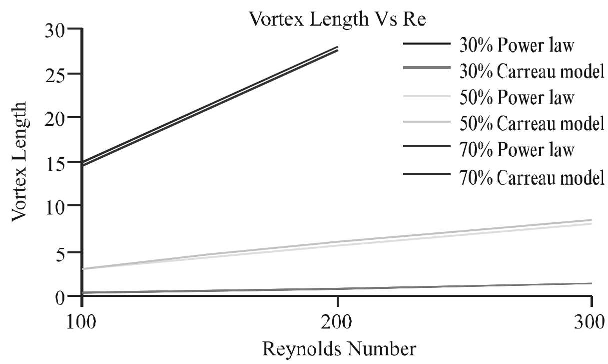

FIG. 1. REATTACHMENT LENGTH AT DOWNSTREAM AGAINST REYNOLDS NUMBERS FOR VARIOUS DEPOSITION LEVELS

TABLE 1. EQUATIONS FOR REATTACHMENT LENGTH (R_l) AT DOWNSTREAM AGAINST REYNOLDS NUMBERS (Re) FOR DIFFERENT PERCENTAGES OF DEPOSITION

Deposition (%)	Equation
30	R_l=4.7x10^{-3} (Re)-0.2187
40	R_l=1.1x10^{-2} (Re)-0.0867
50	R_l=2.35x10^{-2} (Re)+0.1707
60	R_l=4.85x10^{-2} (Re)+0.308
65	R_l=6.78x10^{-2} (Re)+0.272
70	R_l=9.08x10^{-2} (Re)+0.468

TABLE 2. EQUATIONS FOR REATTACHMENT LENGTH AT DOWNSTREAM AGAINST DEPOSITION (D_p) FOR DIFFERENT REYNOLDS NUMBERS

Reynolds number	Equation
50	R_i=2.8x10^{-3} $(D_p)^2$-1.691x10^{-1} (D_p)+2.5497
100	R_i=5.8 x10^{-3} $(D_p)^2$-3.563x10^{-1} (D_p)+5.7898
150	R_i=9x10^{-3} $(D_p)^2$-5.655x10^{-1} (D_p)+9.551
200	R_i=1.22x10^{-2} $(D_p)^2$-0. 7511 (D_p)+13.446
250	R_i=1.54x10^{-2} $(D_p)^2$-1.0003 (D_p)+17.391
300	R_i=1.75x10^{-2} $(D_p)^2$-1.1131 (D_p)+19.126

blood is of logarithmic trend at low values of Reynolds numbers and turns to be nonlinear and reaches at plateu level for very high Reynolds numbers. Whereas, in Table 3 developed empirical equations have been displayed. In contrast to recirculation flow rate of blood against Reynolds numbers, it is computed against blockage and placed in terms of equations, displayed in Table 4, which presents the trend of second order polynomial in Fig 3-5.

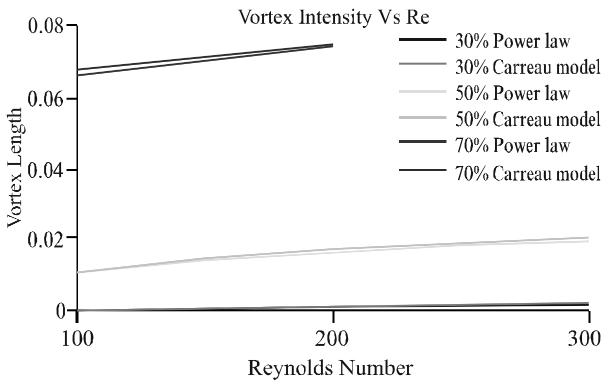

FIG. 2. RECIRCULATION FLOW RATE AT DOWNSTREAM AGAINST REYNOLDS NUMBERS FOR DIFFERENT PERCENTAGES OF DEPOSITION

TABLE 3. EQUATIONS FOR RECIRCULATION FLOW RATE (R_f) AT DOWNSTREAM AGAINST REYNOLDS NUMBERS FOR DIFFERENT PERCENTAGES OF DEPOSITION

Deposition(%)	Equation
30	R_f=0.001 ln (Re)-0.0044
40	R_f=0.0047 ln (Re)-0.0185
50	R_f=0.0092 ln (Re)-0.0309
60	R_f=0.0135 ln (Re)-0.0309
65	R_f=0.0185 ln (Re)-0.0385
70	R_f=0.0171 ln (Re)- .0052

TABLE 4. EQUATIONS FOR RECIRCULATION FLOW RATE AT DOWNSTREAM AGAINST DEPOSITION FOR DIFFERENT REYNOLDS NUMBERS

Reynolds number	Equation
50	$R_f=6\times10^{-5}\ (D_p)^2-\ 5\times10^{-3}\ (D_p)+9.37\times10^{-2}$
100	$R_f=7\times10^{-5}\ (D_p)^2-\ 4.8\times10^{-3}\ (D_p)+8.75\times10^{-2}$
150	$R_f=6\times10^{-5}\ (D_p)^2-\ 4.6\times10^{-3}\ (D_p)+8.04\times10^{-2}$
200	$R_f=6\times10^{-5}\ (D_p)^2-\ 4.4\times10^{-3}\ (D_p)+7.62\times10^{-2}$
250	$R_f=6\times10^{-5}\ (D_p)^2-\ 4.4\times10^{-3}\ (D_p)+7.64\times10^{-2}$
300	$R_f=6\times10^{-5}\ (D_p)^2-\ 4.2\times10^{-3}\ (D_p)+7.25\times10^{-2}$

8. CONCLUSION

The numerical predictions for the flow of blood structure in plaque deposited capillary segment are compared only qualitatively against those available, as complete experimental data in open literature is unavailable. Hence,

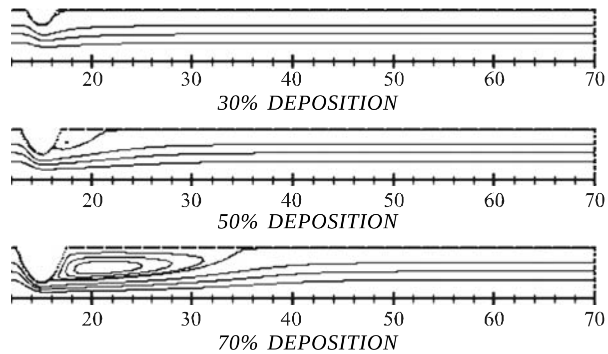

FIG. 3. STREAM-LINE PROJECTIONS FOR PTT MODEL AT REYNOLDS NUMBER Re=100 FOR DIFFERENT LEVELS OF DEPOSITION

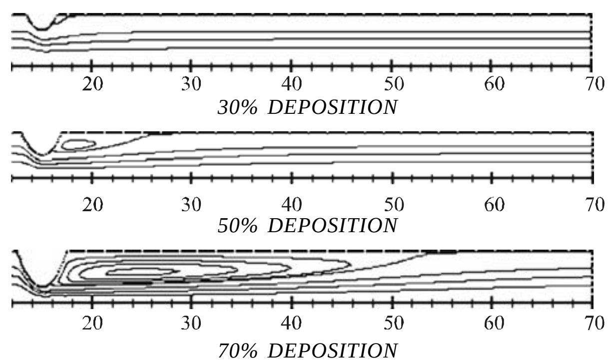

FIG. 4. STREAM-LINE PROJECTIONS FOR PTT MODEL AT REYNOLDS NUMBER Re=200 FOR DIFFERENT LEVELS OF DEPOSITION

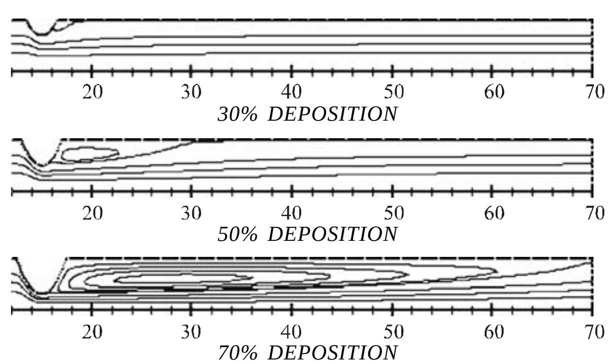

FIG. 5. STREAM-LINE PROJECTIONS FOR PTT MODEL AT REYNOLDS NUMBER Re=300 FOR DIFFERENT LEVELS OF DEPOSITION

numerical simulations are performed for low values of elasticity and the numerical predictions are compared qualitatively against inertial and extensional effects on vortex development. In comparison to Newtonian behaviour of blood, the flow of blood develops vortices in the downstream of the artery segment that grow with increasing inertia as well as various levels of deposition. The formation of vortex from streamline patterns observed that at 30% deposition level is small, moderate at 50% and dominates at 70% level of deposition at downstream of the capillary segment. Since the model has been investigated at low value of elasticity, the computed results on viscoelasticity are observed similar flow phenomenon with the Newtonian case of blood. This is due to the dominancy of inertia, Weissenberg number do not show any marked effect on computed results.

ACKNOWLEDGMENTS

Authors greatly acknowledge with thanks to the HEC (Higher Education Commission, Islamabad, Pakistan, for financial support through project No. 20-217/R&D/2003/615 under National Research Programme for Universities.

REFERENCES

[1] Fung, Y.C., "Biomechanics: Mechanical Properties of Living Tissues", Springer Verlag, 1993.

[2] Oldroyd, J.G., "On the Formulation of Rheological Equations of State", Procedings of Royal Society, Volume A200, pp. 523-541, 1950.

[3] Petrie, C.J.S., "Elongational Flows: Aspects of the Behaviour of Model Elastic Viscous Fluids", Pitman, London, 1979.

[4] Crochet, M.J., Davies, A.R., and Walters, K., "Numerical Simulation of Non-Newtonian Flow", Rheology Series, Volume 1, Elsevier Science Publication, Amsterdam, 1984.

[5] Ikbal, Md. A., Chakravarty, S., and Mandal, P.K., "Unsteady Response of Non-Newtonian Blood Flow through a Stenosed Artery in Magnetic Field", Journal of Computational and Applied Mathematics, Volume 230, pp. 243-259, 2009.

[6] Mandal, D.K., Manna, N.K., and Chakrabarti, S., "A Numerical Model Study of Steady Flow through Bell Shaped Stenosis with and Without Symmetry", International Journal of Experimental and Computational Biomechanics, Volume 1 , pp. 306-331, 2010.

[7] Perera, G.M., and Walters, K., "Long Range Memory Effects in Flows Involving Abrupt Changes in Geometry: Part-2: The Expansion/Contraction/Expansion Problem", Journal of Non-Newtonian Fluid Mechanics, Volume 2, pp. 353-365, 1977.

[8] Pak, B., Cho, Y.I., and Choi, S.U.S., "Separation and Reattachment of Non-Newtonian Fluid Flows in a Sudden Expansion Pipe", Journal of Non-Newtonian Fluid Mechanics, Volume 37, pp. 175-199, 1990.

[9] Mekheimer, Kh.S., and Elkot, M.A., "The Micropolar Fluid Model for Blood Flow through a Stenotic Arteries", International Journal of Pure and Applied Mathematics, Volume 36, pp. 393-405, 2008.

[10] Bird, R.B., Stewart, W.E., and Lightfoot, E.N., "Transport Phenomena", 2nd Edition, John Wiley & Sons, 2002.

[11] Van, K.J., "A Second Order Accurate Pressure Correction Scheme foe Viscous Incompressible Flow", SIAMJ. Science Statistics Company, Volume 7, pp. 870-891, 1986.

[12] Townsend, P., and Webster, M.F., "An Algorithm for the Three Dimensional Transient Simulation of Non-Newtonian Fluid", Theory and Applications, Proceedings of Numeta Conference on Numerical Methematics Engineering, T12/1-11, Nijhoff, 1987.

[13] Townsend, P., and Walters, K., "Expansion Flows of Non-Newtonian Liquids", Chemical Engineering Science, Pergamon, Elsevier, Volume 49, pp. 749-763, 1994.

[14] Baloch, A., and Webster, M.F., "A Computer Simulation of Complex Flows of Fibre Suspensions", Computers Fluids, Volume 24, pp. 135-151, 1995.

[15] Hawken, D.M., Tamaddon, Townsend, P., and Webster, M.F., "A Taylor-Galerkin Based Algorithm for Viscous Incompressible Flow", International Journal of Numerical Methematics Fluids, Volume 10, pp. 327-351, 1990.

[16] Walters, N.D., and King, M.J., "Unsteady Flow of an Elastico-Viscous Liquid", Rheology Acta, Volume 9, pp. 345-355, 1970.